Available online at www.sciencedirect.com

ScienceDirect

Procedia CIRP 110 (2022) 87–92

www.elsevier.com/locate/procedia

V CIRP Conference on Biomanufacturing

A Computational Model For The Design Optimization Of Multi-Electrode Arrays By Aerosol-Jet Printing

Ileana Armando[a]*, Michela Borghetti[a], Emilio Sardini[a], Mauro Serpelloni[a]

[a]*Department of Information Engineering, University of Brescia, Via Branze 38, 25123 Brescia, Italy*

* Corresponding author. Tel.: +39 030 - 3715938. *E-mail address:* i.armando@unibs.it

Abstract

The microelectrode arrays (MEAs) have become a valuable tool in the study of electrophysiological analysis of *in vitro* electrogenic cells. Aerosol-Jet Printing (AJP) is an alternative to traditional fabrication technique. AJP allows the development of flexible and customized devices. Here we present a computational modelling method using Comsol Multiphysics, to enhance the design optimization of printed microelectrode array. The computational outcomes lead to the identification of the optimal microelectrode array design considering the main requirements of fabrication MEA and the intrinsic limitations of the Aerosol-jet printing technique.

© 2022 The Authors. Published by Elsevier B.V.
This is an open access article under the CC BY-NC-ND license (https://creativecommons.org/licenses/by-nc-nd/4.0)
Peer-review under responsibility of the scientific committee of the V CIRP Conference on Biomanufacturing

Keywords: Microelectrode Array; Aerosol Jet Printing; Computational Model; Comsol Multiphysics; *in vitro* electrophysiology.

Nomenclature

MEA	MicroElectrode Array
AJP	Aerosol Jet Printing
C_m	membrane capacitance [F]
i_{Na}	Na^+ ionic current [A]
i_K	K^+ ionic current [A]
i_L	non-specific leakage current [A]
g_{Na}	Na^+ ionic conductance [S]
g_K	K^+ ionic conductance [S]
g_L	non-specific leakage conductance [S]
i_s	stimulus current amplitude [A]
t_{on}	onset time [s]
t_{dur}	duration of the stimulus [s]
V	transmembrane potential [V]
V_{Na}	reversal potential for Na+ membrane current [V]
V_K	reversal potential for K membrane current [V]
V_L	reversal potential non-specific leakage membrane current [V]
J	total current flux [A/m^2]
Je	externally generated current density [A/m^2]
σ	electrical conductivity of the material [Ω·m]
Q	total charge enclosed within the V [C]
D	electric displacement [C/m^2]
ϵ_0	vacuum permittivity [F/m]
ϵ_r	relative permittivity

1. Introduction

Microelectrode arrays (MEAs) are widely used to study the electrophysiological activity of *in vitro* of cells. Such devices are composed of a grid of tightly spaced electrodes employed to record and stimulate the electrogenic cells. Furthermore, MEAs are a key component in several applications, from *in vitro* toxicity studies to implantable brain-machine interface. They are employed to acquire extracellular signals and affect the properties of the measured electrical signals significantly, including the shape of the waveforms. The recording of the action potential generated by the electrical potential of cells would help to identify the electrophysiological behaviour, e.g.,

2212-8271 © 2022 The Authors. Published by Elsevier B.V.
This is an open access article under the CC BY-NC-ND license (https://creativecommons.org/licenses/by-nc-nd/4.0)
Peer-review under responsibility of the scientific committee of the V CIRP Conference on Biomanufacturing
10.1016/j.procir.2022.06.018

This is a resupply of March 2023 as the template used in the publication of the original article contained errors. The content of the article has remained unaffected.

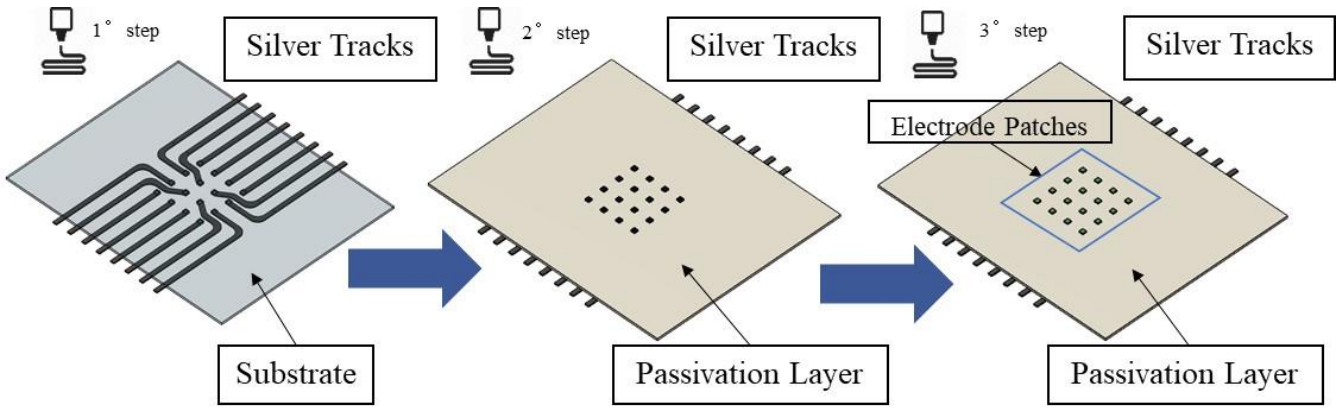

Figure 1. Rendering of the process fabrication with Aerosol Jet Printing of the three steps.

the analysis of neuronal action potential, and the configuration in designing bioelectric systems for the detection and assessment of cells and for the standardization and automation of tissue engineering processes. These developments are crucial for the evolution of automated cell and tissue handling and assessment in future bioreactors [1,2]. Nowadays, the microfabrication of common MEAs allow dimension of 10-100 μm and metal material as electrode patches but are expensive concerning time and cost production. This leads to reuse and extending the lifetime of the microelectrode with a decrease in the quality of the recorded signals. Therefore, the need for an alternative production technique remains to overcome these limitations. Recently, printing techniques have been increasingly used in electronic devices, as a promising strategy to achieve customized and low-cost production. Aerosol Jet Printing (AJP) is a feasible technique that allows printing different inks on a wide range of substrates. Furthermore, small droplets dimensions and performance achievable allow printing object of micro dimension. The technique provides a selective deposition both on planar and 3D structures, without using masks or post-processing, and realizing specific surface features. Furthermore, printing technologies have enabled the evolution of printed and flexible electronics and the use of conductive polymers such as PEDOT-PSS, a polymeric material that has excellent properties in terms of conductivity, processability, and stability. For biomedical applications, it shows good biocompatibility and is used a coating for the metallic material to improve the signal-to-noise ratio (SNR) of the recorded signals and the increase of the surface area [3,4].

The use of computational modelling method for the design and analysis of bioelectronic devices enable efficient exploration of large parameter sets, e.g., geometrical setup and electrical and multiphysic parameters, where preclinical and clinical studies would not be feasible. The 3D finite element method (FEM) simulation can connect the model with the measurement environment, allowing the analysis of the recorded data regarding the geometry setup. Proper electrical characteristics of the MEA, cell culture medium, and cells, need to be employed to achieve proper conclusions to assess a realistic model of the device. To this end, FEM has been used to analyse cell–electrode connections affecting the electrical stimulation and recording of cells, cell growth, and cell–electrode interfaces in general. Such simulations provide predictions of measurement values but lead to some limitations due to the simplified model. To study various measurement arrangements about biological matter, new simulation methods, such as those proposed in this paper, are called for. The FEM simulation enables the analysis of different design setup to find the ideal result. In silico models are a valid tool to predict the behaviour of neuronal cell activity [5, 6, 7].

In this paper, we propose the application of computational simulation methodology in terms of distribution of the electrical potential analysis of action potential of neuronal cells. The aim is to obtain an optimization of the design of printed microelectrode array that is intended to be fabricated with the AJP technique. The study includes the realization of a model to predict the microelectrode array performance through the evaluation of the electrode detection area and the ideal insulated layer thickness to avoid crosstalk of recording signals.

2. Material and method

2.1. Fabrication design

The micro-electrode array (MEA) design involves the realization of an array of 4x4 electrodes of 50 μm with a total distribution of the recording sensitive area of 1-2 mm^2. According to the literature [2], the electrode dimension must be comparable to the cell dimension. While interelectrode distance has to be major to the cell dimension, considering the electrode geometry range and according to intrinsic AJP requirement, the inter-electrode distance is necessarily between 200 to 300 μm. The fabrication process decision, in addition to the geometry set-up, is relevant for the computational model in terms of thickness of the different layer deposition and the main geometry parameters such as electrode dimension and interelectrode distance. In this work, as seen in Fig.1 and Fig.2

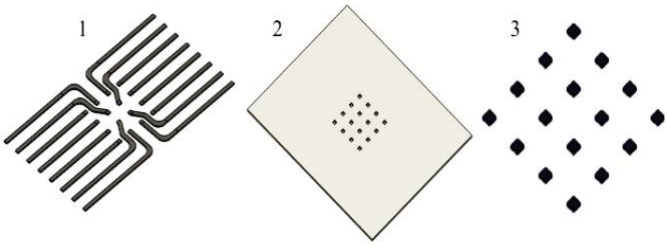

Figure 2. Rendering of the three layers of the microelectrode array. 1) 16 silver tracks for the conduction of the signal, 2) Insulating layer in Norland Optical Adhesive (NOA) and 3) 16 electrode patches in PEDOT-PSS.

This is a resupply of March 2023 as the template used in the publication of the original article contained errors. The content of the article has remained unaffected.

the fabrication process of MEA, using Aerosol-Jet Printing (AJ300, Optomec, Albuquerque, NM, USA), is composed of three steps to realize the different layers geometries of the electrode array. The first layer of silver (Ag) is printed on the substrate, the silver has been chosen for the high conductive properties. The first layer has to deliver the signal to the electronic hardware. The passivation layer, as a coating to the silver track, is printed with an insulating layer, Norland Optical Adhesive (NOA). Besides having low conductivity, it is transparent and biocompatible material. Finally, since AJP technique allows to print conductive polymers, Poly(3,4-ethylenedioxythiophene)-poly(styrenesulfonate) (PEDOT-PSS) has been chosen as a surface coating for the leaving opening at the end of the silver lines of the first layer and to realize the contact pads with conductive polymer to obtain an increased signal to noise ratio (SNR) and better biocompatibility and more surface area incrementation.

2.2 Computational method

Once MEA set-up has been designed and the printing process defined, it is necessary to carry out several simulations aimed at evaluating some project specifications that need to be improved, to obtain an enhanced fabrication process and an optimized design. The finite element method (FEM) models of the AJP microelectrodes, cells, and culture medium are developed and implemented in COMSOL Multiphysics (COMSOL, Inc., Burlington, MA, USA). The tool was used to compute the evaluation of the ideal insulated layer thickness to avoid crosstalk of recording signals and the design enhancement of MEA according to the aerosol jet printed requirements to assess the detection area of the electrodes.
We constructed a 3D model with planar square electrodes on the surface of the insulating substrate, as in the commercial MEAs, with a cell immersed in culture medium in Fig. 3. The position of the cell was changed in various locations in the proximity of the electrodes to assess different simulations parameters. Furthermore, to compute the crosstalk evaluation, in addition to the electrodes and the insulating substrate, another domain that represent the conductive silver tracks is added to the domains.
Regarding the single domain representation, the neuronal cell was modelled as an adherent cell to the MEA substrate surrounded by culture medium. The typical radius of the soma of a human neuron is between 7 to 20 μm. Here, we assumed a neuronal cell of 15 μm radius. In addition, the cell was assumed

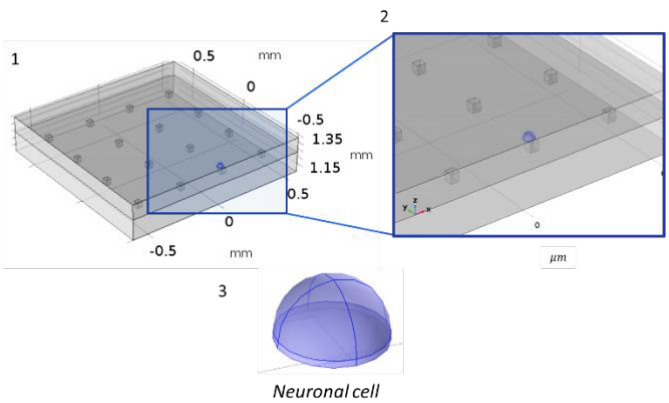

Figure 3. Geometry model of MEA, cell culture medium and 3) neuronal cell.

without axons and dendrites and thus propagation signal to reduce the computational cost and complexity.
The electric properties of the various domains used in the Comsol simulation are reported in Table 1. Comsol material database provided the electrical properties of silver material, in terms of relative permittivity and electrical conductivity. The specific electric properties of the other domain were set according to the electrical parameters reported in the literature [7]. Considering the insulating layer, the Norland Optical Adhesive properties had a crucial importance in the simulations and the MEA realization due to its function in the passivation layer, and the electrical conductivity was set $9.09*10^{-9}$ S/m.

Table 1. Electrical parameters for the different material domains used in the simulations

Material domain	Relative permittivity	Electrical conductivity (S/m)
Medium	80	3
Cell Membrane	11.3	$1*10^{-24}$
Silver (Ag)	1000	$5.99*10^{7}$
PEDOT-PSS	100	5e4
Norland Optical Adhesive (NOA)	3.2	$9.09*10^{-9}$

The electric currents module was imposed as physics in COMSOL Multiphysics to calculate the electric fields and the electric potential distributions in the entire volume of the model and across the insulating layer associated with the analyzed electrode configurations. In particular, for numerical modeling of the coupling between the cell and the MEA, Maxwell's equations were used. These equations are represented in the differential form of Gauss's law to model electric current flow in conductive and capacitive medium and solve a current conservation problem. The stationary equation of continuity must be considered for stationary electric currents in conductive media.
The Ohm's law is:

$$J = \sigma \cdot E + Je \quad (1)$$

Where J = total current flux, Je = externally generated current density, σ = electrical conductivity of the material.
The utilized physics solves the equations based on the Ohm's law using the electrical potential as dependent variable. Gauss's law for electric charge distribution to handle current sources, the static form of the equation of continuity can be generalized:

$$\nabla \cdot J = Qj, v \quad (2)$$

Q = total charge enclosed within the V.
Dielectric model for macroscopic properties of the model:

$$D = \epsilon_0 \cdot \epsilon_r \quad (3)$$

Where D is the electric displacement, ϵ_0 is the vacuum permittivity and ϵ_r is the relative permittivity.
Based on Gauss's law for electrical field and Ohm's law, electrical potential distribution in each domain of the system was calculated by the COMSOL software. The electrical insulation boundary condition is defined as

This is a resupply of March 2023 as the template used in the publication of the original article contained errors. The content of the article has remained unaffected.

$$n \cdot J = 0 \qquad (4)$$

The boundary conditions concern the current conservation on all the domains and the electric insulation on all the boundaries. A potential difference according to action potential signal was fed in the surface via terminal at the entire cell surface, while all the external domain boundaries were set to ground. The array of microelectrode was used to record the propagation of the action potential signal around the cell, specifically the distribution of electrical potential in the electrode domain. The simulation was set with a time-dependent step between 0 to 0.02 s, the duration of a single spike of the action potential, and the consequence refractory period. The input signal was fed as a terminal for the generation of the electrical potential and consequently, the signal recorded by the microelectrode array for neuronal cells is the action potential signal, a potential difference between the outside and inside of the membrane. The difference in the concentration of ions between the inside and outside through the membrane of the cell leads to membrane potential. Such potential difference changes over time, starting from a resting potential of -70 mV to a rapid depolarization, positive membrane potential with a peak of 50 mV and subsequently, repolarization of the membrane. Finally, a refractory period leads to resting potential. For the generation of the action potential of the neuron provided as an electrical potential input to the cell membrane presented in this work, the model of Hodgkin–Huxley was chosen. The mathematical model of the neural electrical activity is based on their electrophysiological experiments in the giant axon of the squid [8]. The neuron was represented as a single compartment, ignoring any spatial propagation in electrical activity. The neural membrane is described in Fig. 4 by a capacitance *Cm* in parallel with three conductance.

$$i_{Na} = g_{Na}(V - V_{Na}) \qquad (5)$$
$$i_K = g_K(V - V_K) \qquad (6)$$
$$i_L = g_L(V - V_L) \qquad (7)$$

$$C_m \frac{dV}{dt} = -(i_{Na} + i_K + i_L) \qquad (8)$$

C_m= membrane capacitance
i_{Na} = Na+ ionic current
i_K = K+ ionic current
i_L= non specific leakage current
g_{Na}= Na^+ ionic conductance [S]
g_K= K^+ ionic conductance [S]
g_L= non-specific leakage conductance [S]

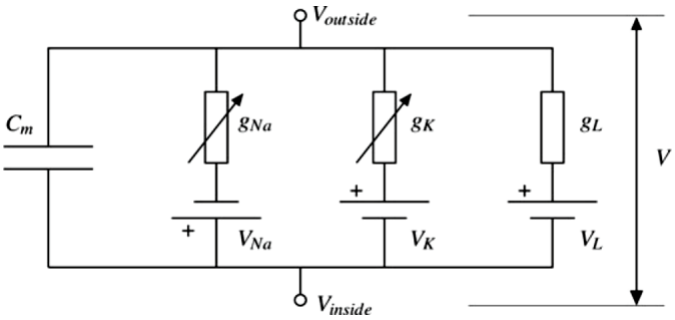

Figure 4. Modelling of the neural cell membrane.

V= transmembrane potential
V_{Na} = reversal potential for Na+ membrane current
V_K = reversal potential for K+ membrane current
V_L = reversal potential for non-specific leakage membrane current. Hodgkin–Huxley neuron model [8] responds to a brief stimulus, shown in the membrane potential V against time. Using a square-wave profile, this stimulus current is given by

$$i_{stim} = \begin{cases} i_s & t_{on} \le t < t_{on} + t_{dur} \\ 0 & otherwise \end{cases} \qquad (9)$$

In the specific case of the simulation reported in this work, the values assigned are:
i_s= 600 A/m^2
t_{on} = 0.001 s
t_{dur}= 0.001 s
The resulting action potential on the cell membrane according to the values assigned is shown in Fig. 5 with a peak with an amplitude of 50 mV after 0.002 s, the duration of a single impulse is about 0.02 s. Finally, the mesh allows the discretization of the model, using the finite element method that divides the model into elements with a simple geometrical shape. An extra fine mesh is imposed to improve the computation accuracy, but this leads to increased memory usage and a reduced speed.

3. Results

3.1 Evaluation of the simplified model

The results of Comsol simulations in Fig. 6 show the electrical potential distribution of the geometry composed of a microelectrode array (electrode, insulating layer, and conductive tracks), cell and medium. The orange signal is the action potential input of the cell membrane, peaks at 50 mV while the blue waveform is the signal recording of electrical potential by the electrode when the cell is located at 80 μm (Fig. 6a) and at 30 μm (Fig. 6b) along x-axis. The figure shows how the action potential profile is recorded by the electrode; meanwhile, the field intensity of the signal decreases with the distance from the electrogenic cell according to the inverse square law of electricity [9]. Compare to Appali [10], which uses a model with a higher level of complexity in terms of geometry domains and the physics that use a ramification cell model and propagation of the action potential, we modelled the

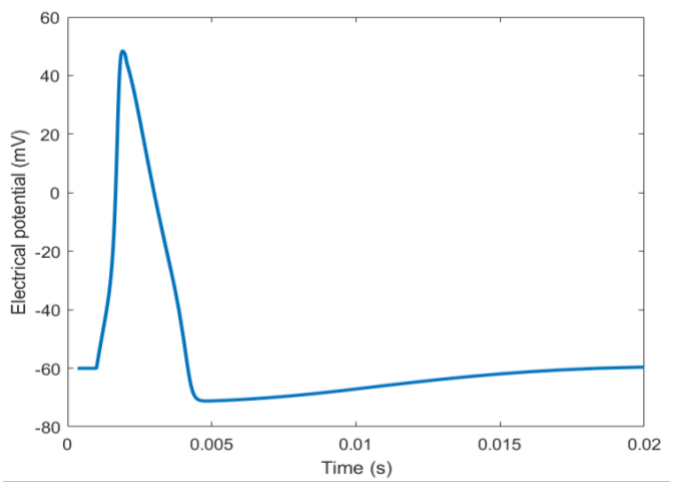

Figure 5. Action potential of a neuronal cell.

This is a resupply of March 2023 as the template used in the publication of the original article contained errors. The content of the article has remained unaffected.

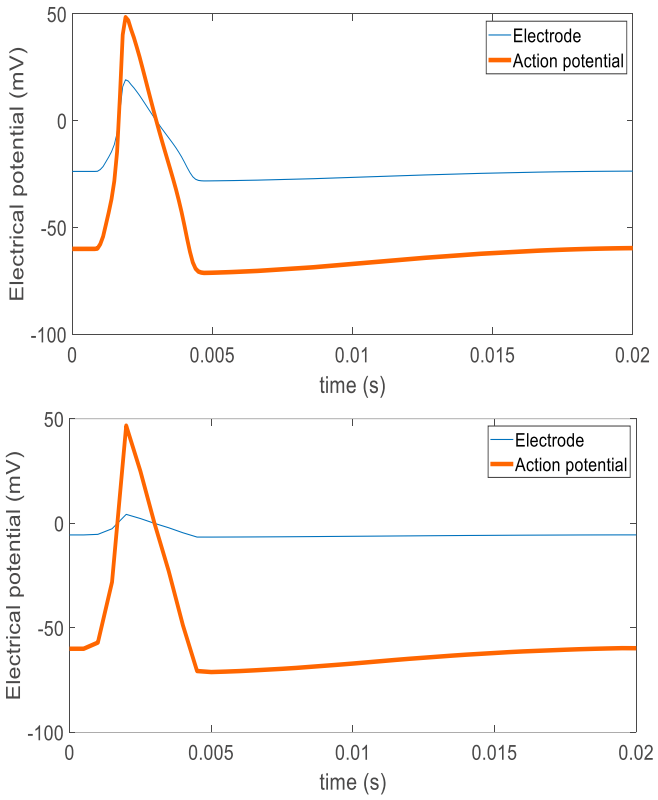

Figure 6. Plot of the action potential signal and recorded signal by the electrode at distance between them of a) 80 μm and in b) 30 μm.

action potential with a simplified physics, a single imposed stimulus and a cell geometry composed of a single cell with hemispherical shape. In spite of the simplification of the model presented in this work, our simulation reported a proper rendering in terms of profile recording and signal decrease according to the distance.

3.2 Assessment of the detection area of MEA

Comsol Multiphysics was applied to compute the detection area for the electrode array. We estimated the distribution of the electrical potential delivered according to the position of the cell according to the electrode array. It allows assessing the correlation between cell and electrode distance. The plot shows on the y-axis the amplitude peak of the cell action potential recording from the electrode, assuming the diameter of 50 μm, while the position of the electrode is plotted on x-axis. For the evaluation of the detection area of the electrode, the spike of the action potential was taken into account, i.e. the electrical potential peak at which the maximum potential difference is reached during a single 50 mV peak stimulus. The plot in Fig. 7 shows how the distance between electrode and cell influences the action potential recording. The plot was obtained from several simulations carried out by moving the neuronal cell along the x-axis. The electrode is in the origin position. The detection field results the highest in the area close to the center of the electrode at x=0, as expected. Due to the size of the cell (of 30 μm diameter), the area of major sensitivity is extended. Moving away from the electrode, the sensitivity rapidly decreased as can be seen in the Fig. 7. The presence of the cell near the electrode of 10 μm provides a decrease of the signal of 20 mV. At distances x >20 µm from electrode in the x-direction, sensitivity drops below 40%, and down to 10% at x = 30 µm. The detection area decreases very fast as shown in the image, and the recording signal is about 2 mV with a cell-electrode distance of 100 μm. The signal equal to 0 for a distance more than 150 μm, it means that the action potential is no longer detectable for distances larger than 150 μm. As seen from Fig. 7, the measurement sensitivity of an electrode setup is positive in the entire analyzed area, and maximum at the center of the electrodes where the electrical potential is the highest due to the position of the cell on the top of the electrode. According to Fig. 7, the cell in the proximity of the microelectrode caused an increase of the potential, leading to an increase of the recording signal. The electrical potential and the recording signal from the electrode increase depending on the location of the cell. The definition of a single electrode detection area leads to an analyze of the cross-sensitivity of two electrode configuration to investigate the interelectrode distance to achieve the optimal MEA design. Concerning the design requirements of the microelectrode array, the ideal distance between two consecutive electrodes is greater than the neuronal cell diameter, and concurrently the gap should not exceed in order to avoid areas where the action potential signal is not recorded by the sensors. Due to the intrinsic limitation of the printed MEA, the minimum interelectrode distance achievable is 200 μm. We estimated the electrical potential distribution with two-electrode configuration at the chosen distance, based on the Comsol Multiphysics simulation carried out. The Fig. 8 shows the cross-detection area of two electrodes, and the behaviour is the same of the configuration of the single electrode. It is interesting to observe what happens in the cross-detection area, the minimum recorded signal that can be detected from the sensor is 2 mV, due to the

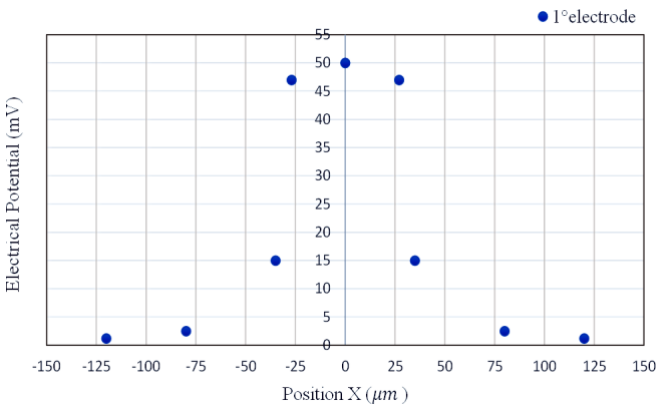

Figure 7. Detection field of the single electrode configuration without a cell visualized. The electrode is localised in the x-y origin.

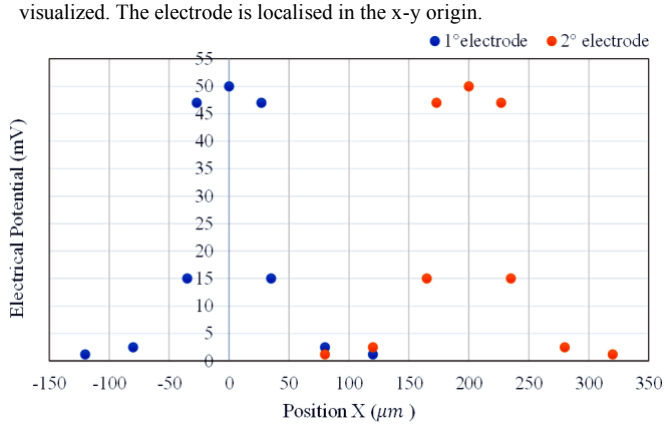

Figure 8. Detection field of the two electrode configurations without cell visualized. The 1° first electrode is localized in the x-y origin and the 2° electrode at 200 μm away.

This is a resupply of March 2023 as the template used in the publication of the original article contained errors. The content of the article has remained unaffected.

interelectrode distance of 200 μm. An increase of the interelectrode distance more than 200 μm would result in a detection area in which the signal is no more recordable.

3.3 Evaluation of the Insulated layer thickness

The extracellular electrode can record the field potential generated by the action potential of more neurons *in vitro*. The recorded signal reflects the spike of individual neurons and low field potential and synaptic potentials. Therefore, it is necessary to reduce the possible additional noise, such as the interference crosstalk signal between the several action potentials and the conductive tracks in silver that can be generated by a non-adequate insulated layer thickness. For such reason, the width of the insulating layer must be studied to avoid crosstalk between the signal recording by the electrode and the interference between external action potential signals and conductive path. Several simulations are performed to evaluate the optimal compromise between layer thickness from AJP requisite and crosstalk limitations. The thickness values are chosen as follow: for the inferior limit, 10 μm was chosen because it is the minimum layer thickness that can be printed with AJP with the NOA and for the superior, we tested 300 μm. The results obtained for the different layer thickness regard the entire action potential signal. The Fig. 9 shows how the variations of the electric potential for 10 μm of thickness differ by 1% from 300 μm. Therefore, the variation of the potential is not relevant to interfere with the signal of the recording electrode.

4. **Conclusion**

Due to the importance of understanding electrophysiological signals of electrogenic cells, the microelectrode array is crucial in biomedical research and its subsequent use as a tool for the assessment of cellular viability. It is fundamental the optimization and the customization of the microelectrode array design to produce bioelectronic devices able to lead to an improvement of the knowledge in the tissue engineering field. The employment of new printed manufacturing techniques allows the production of customized and, cost and time reduction devices. Besides the possibility of using polymeric materials lead to better results in terms of signal quality and biocompatibility. In the specific, before proceeding with the realization of an electrode array device, it is necessary to design the set-up and the electrical parameters to obtain the achieved result, and this is possible due to the use of computational techniques. In this work, we demonstrated the importance of the FEM model for the optimization of the design for a new fabrication technique for the realization of microelectrode array which involves the use of Aerosol Jet Printing. The detection area analysis of the electrode array for the recording of the action potential of neuronal cells led to the definition of an interelectrode distance of 200 μm. Furthermore, according to the intrinsic requirements of AJP and the results obtained from Comsol simulation, the evaluation of the insulating layer thickness led to an optimal thickness of Norland Optical Adhesive used as passivation layer of 10 μm, because such value do not lead to an undue noise concerning the electrical potential signal recording by the electrode.

In conclusion, the system used in the simulation is necessarily ideal, including the assumed geometry, e.g. the neuronal network is assumed as a single neuron with hemispherical shape and the propagation of the action potential is negligible. Nevertheless, a well-defined and simplified geometry in the MEA system is necessary to achieve a basic understanding of the action potential measurement and bioelectronic device. Although the concepts and the results obtained from the simulation will assess the design optimization considering the geometry set-up and electrode dimensions for microelectrode array. These simulations can be used for the analysis of stimulation and recording of electrodes qualitatively. The model is a good compromise of computational power and model predictability. The future works will include the realization of the printed microelectrode array by Aerosol Jet Printing according to the computational results achieved.

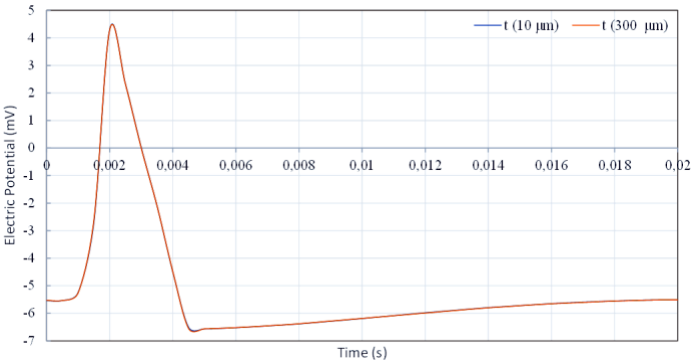

Figure 9. Action potential signal from the recorded electrode with an insulating layer of 10 μm and 300 μm.

References

[1] Kim, G. H., Kim, K., Lee, E., An, T., Choi, W. S., Lim, G., & Shin, J. H. (2018). Recent progress on microelectrodes in neural interfaces. Materials, 11(10). https://doi.org/10.3390/ma11101995

[2] Xu, L., Hu, C., Huang, Q., Jin, K., Zhao, P., Wang, D., … Ma, H. (2021). Trends and recent development of the microelectrode arrays (MEAs). Biosensors and Bioelectronics, 175(88), 112854. https://doi.org/10.1016/j.bios.2020.112854

[3] Garma, L. D., Ferrari, L. M., Scognamiglio, P., Greco, F., & Santoro, F. (2019). Inkjet-printed PEDOT: PSS multi-electrode arrays for low-cost: In vitro electrophysiology. Lab on a Chip, 19(22), 3776–3786. https://doi.org/10.1039/c9lc00636b

[4] Serpelloni, M., Cantù, E., & Borghetti, M. (2020). Printed Smart Devices on Cellulose-Based Materials by means of Aerosol-Jet Printing and Photonic Curing.

[5] Dokos, S. (2017). Modelling organs, tissues, cells and devices using Matlab and Comsol multiphysics. Berlin: Springer.

[6] Böttrich, M., Tanskanen, J. M. A., & Hyttinen, J. A. K. (2017). Lead field theory provides a powerful tool for designing microelectrode array impedance measurements for biological cell detection and observation. BioMedical Engineering OnLine, 1–17. https://doi.org/10.1186/s12938-017-0372-5

[7] Taghian, T., Narmoneva, D. A., & Kogan, A. B. (2015). Modulation of cell function by electric field: A high-resolution analysis. Journal of the Royal Society Interface, 12(107), 21–25. https://doi.org/10.1098/rsif.2015.0153

[8] A. L. Hodgkin, A. F. Huxley, A quantitative description of membrane current and its application to conduction and excitation in nerve, J. Physiol. London 117 (1952) 500 – 544.

[9] R. Feynman, The Feynman Lectures on Physics, Vol. 2, (Addison-Wesley, Boston, (1963).

[10] Appali, R. (2014). Modeling the coupling of action potential and electrodes. University of Rostock, Germany

This is a resupply of March 2023 as the template used in the publication of the original article contained errors. The content of the article has remained unaffected.